
PAIR: Prefix-Aware Internal Reward Model for Multi-Turn Agent Optimization

Wonjoong Kim¹, Yeonjun In¹, Sangwu Park¹, Dongha Lee², Chanyoung Park^{1*}

¹KAIST ²Yonsei University

{wjkim, yeonjun.in, sangwu.park, cy.park}@kaist.ac.kr
donalee@yonsei.ac.kr

Abstract

A significant hurdle for current LLMs is the execution of complex, multi-stage tasks. Group Relative Policy Optimization (GRPO) has been emerging as a leading choice, but its reliance on sparse outcome rewards severely limits credit assignment across intermediate steps. Existing remedies—running full rollouts to assign step-level advantages, calling external LLM judges at each step, or computing intrinsic rewards that require ground-truth answers at every evaluation—introduce significant costs or practical constraints. We hypothesize that internal correctness probing over LLM hidden states can be repurposed as a step-level reward signal, potentially addressing all of these limitations at once. However, existing probing research assumes clean inputs, and we first show that this assumption breaks down in multi-step settings: hidden-state probes degrade severely under prefix contamination—tracking coherence with the (possibly corrupted) prefix rather than grounded correctness—while attention-based features remain robust to contamination but underperform on clean prefixes. Building on this complementary relationship, we propose the Prefix-Aware Internal Reward (PAIR)—a two-stage model with a frozen hidden-state probe estimating belief-consistency and a lightweight attention-based head correcting it toward grounded correctness. Experimental results show that PAIR achieves the highest AUROC on contaminated trajectories while operating at negligible inference cost, enabling dense step-level reward signals for GRPO training without external model calls, ground-truth dependencies, or full-trajectory rollouts².

1 Introduction

Multi-step reasoning tasks—where an agent must handle a sequence of actions (e.g., API calls, tool invocations) and interpret environmental feedback before producing a final answer—have emerged as a central challenge for large language models (LLMs). Training LLMs in such settings increasingly relies on reinforcement learning, and Group Relative Policy Optimization (GRPO) [4, 15] is widely adopted due to its simplicity and strong empirical performance. When applied to multi-step agent tasks, however, GRPO operates with only a *sparse outcome reward*—a single scalar indicating whether the final answer is correct. This sparsity makes credit assignment across intermediate steps extremely difficult: the training signal cannot distinguish which steps contributed to success or failure, leading to slow convergence and poor sample efficiency. To mitigate this issue, several lines of work have attempted to introduce denser, step-level reward signals for multi-step agent training, but each comes with notable limitations.

One natural approach for step-level reward signals is to run the model to completion and then propagate the **outcome reward** backward to assign per-step advantages [5, 33]. However, even when early steps are clearly erroneous, the agent cannot know this at generation time and must complete the full trajectory before any signal is available. This produces a large volume of wasteful rollouts from already-failed trajectories, resulting in significant computational inefficiency. An alternative

*Corresponding Author

²Our source code is available at <https://github.com/wonjoong-kim/PAIR>.

Table 1: Comparison between reward mechanisms for GRPO based on their functional requirements.

	Outcome	LLM-based [23]	Tree-based [5, 33]	Intrinsic [17, 25]	PRM [18, 24, 32]	Ours
Dense reward	✗	✓	✓	✓	✓	✓
w.o. LLM	✓	✗	✓	✓	✓	✓
w.o. full rollout	✗	✓	✗	✓	✓	✓
w.o. external func.	✓	✓	✓	✓	✗	✓
w.o. ground-truth	✗	✗	✗	✗	✗	✓

is to query a strong **external LLM** at every step to evaluate that step’s quality. However, judging intermediate steps is inherently difficult, leading to naïve reward criteria (e.g., format validity) and the per-step API cost and latency make this approach impractical for online RL training at scale. Other research leverage the model’s own log-probabilities as a reward signal, but these approaches require the **ground-truth answer** at every reward computation: they calculate teacher-forced log-probabilities of the gold response conditioned on the current trajectory prefix [17, 25]. While training datasets may provide ground-truth answers, the key limitation is that this computation must occur at runtime for every rollout—an operational dependency that restricts applicability and adds non-trivial forward-pass cost. Recent multi-turn RL studies [18, 24, 32] address step-level credit assignment but universally rely on **external reward models**—separately trained networks or LLM judges—rather than leveraging the agent’s own internal representations, incurring significant overhead in training and maintaining these external components.

As illustrated by the comparison in Table 1, there remains a significant gap in achieving a reward signal that is both dense and entirely independent from external models. These limitations raise a natural question: *can we provide dense step-level rewards at every step, without full-trajectory rollouts, without external LLM calls, without ground-truth dependencies at runtime, and without a separate reward model—using only the agent’s own internal states?*

We propose extracting inherently encoded correctness information from an LLM’s internal signals to serve as a dense, step-level reward for GRPO training. This approach is motivated by recent probing research showing that two complementary types of internal signals during generation—*hidden states* [22] and *attention patterns* [2, 11]—implicitly carry information about model’s own correctness. It resolves all four limitations above simultaneously: no full rollouts needed (rewards are computed per step), no external LLM calls (probes run on the agent’s own representations), no runtime ground-truth dependency (probes are trained offline and applied to new trajectories), and near-zero marginal cost. However, applying this idea to multi-step agent settings introduces a fundamental challenge: *prefix contamination*. That is, during RL exploration, the agent inevitably generates erroneous intermediate steps, corrupting the prefix on which subsequent steps are conditioned. To assess whether internal probes remain reliable under such contamination, we conduct a systematic analysis of internal probe behavior under prefix contamination and uncover three findings:

- **Hidden-state probes degrade severely under contamination.** Hidden-state probes degrade severely under contamination because they encode coherence with the (possibly corrupted) prefix rather than grounded correctness, inverting the reward signal at repair turns.
- **Attention features are comparatively robust.** Attention features capture structural behavior and exhibit smaller drops under contamination.
- **The two signals are complementary.** The two signals are complementary: hidden-state dominates on clean prefixes, attention on contaminated ones, neither suffices alone.

Building on these findings, we propose the **Prefix-Aware Internal Reward Model for Multi-Turn Agent Optimization (PAIR)**, a two-stage architecture that preserves the strength of hidden-state probes under clean conditions while correcting their failures under contamination. We get a belief-consistency score s_{bc} from a pre-trained hidden-state probe. An attention-based correction head then takes the attention features together with s_{bc} and predicts a final score s_{final} that adjusts s_{bc} toward grounded correctness, which serves as the step-level reward. By this design, the model learns $s_{final} \approx s_{bc}$ under clean prefixes, where belief-consistency already aligns with grounded correctness, automatically preserving baseline performance. Under contaminated prefixes, on the other hand, the attention-based head activates to correct the divergence. It is worth noting that supervision is required only *once, offline*; at inference time, the model operates at probe-level cost, making it directly usable as a dense step-level reward in GRPO training.

In summary, our main contributions are as follows:

- **Empirical:** We provide the first systematic study of internal correctness probe failure under prefix contamination in multi-step agent settings.
- **Mechanistic:** We demonstrate that hidden states track belief-consistency while attention tracks structural patterns, and that these two signals are complementary—a finding that explains why naïve probes fail and guides the design of robust alternatives.
- **Methodological:** We propose PAIR, which adaptively combines hidden-state and attention signals via a correction architecture, preserving clean-prefix performance while restoring robustness under contamination.
- **Practical:** PAIR operates without external LLM calls, without runtime ground-truth access, and at probe-level inference cost, enabling dense step-level rewards for GRPO training of multi-step reasoning agents.

2 Related Work

2.1 Reinforcement learning for LLM agents

Reinforcement Learning from Human Feedback (RLHF) has become the dominant paradigm for aligning large language models with human preferences. InstructGPT [12], trains a reward model on human preference data and then optimizes the policy against this reward using Proximal Policy Optimization (PPO) [14, 16]. While effective, PPO requires maintaining a value (critic) network of comparable size to the policy network, which substantially increases memory consumption and training cost, and introduces additional instability from value function estimation. Building on this line, Group Relative Policy Optimization (GRPO) [4, 9, 15, 29, 31] removes the value network entirely and instead estimates the baseline from a group of responses to the same prompt, normalizing rewards within each group. This design retains PPO’s clipped surrogate objective while dramatically reducing memory footprint, and has been shown to scale effectively to large reasoning models. However, in multi-turn agentic environments, GRPO faces the sparse outcome reward problem, where the signal is only provided at the completion of a trajectory. This sparsity leads to significant credit assignment challenges, particularly in identifying which intermediate steps contributed to the final success or failure.

2.2 Step-level and process reward models

To mitigate the limitations of sparse rewards, several studies have proposed dense, step-level feedback mechanisms. Process Reward Models (PRMs) provide supervision for intermediate reasoning steps rather than just the final answer [8, 10, 20, 21, 27, 28, 30]. However, extending PRMs to agentic settings—where step correctness is context-dependent and not easily verified—remains challenging [24].

Tree-based Rewards. Methods such as AT²PO [33] and Tree-GRPO [5] utilize tree-search and sibling rollout comparisons to derive step-level advantages. While effective, these methods incur high computational overhead due to the requirement of multiple rollouts per step.

LLM-as-a-Judge. Recent papers try to use an LLM as a judge for correctness, reducing the human cost [3, 7]. Approaches like MT-PPO [23] employ secondary LLMs (e.g., GPT-4) for rule-based evaluation of the quality of each turn. However, the associated API costs and inference latency make them less practical for large-scale online RL training.

Intrinsic and External Rewards. Recent works such as AgentPRM [24] and SWEET-RL [32] have explored multi-turn agent optimization, but they depend on external reward models. Other intrinsic methods like IGPO [17] and TIPS [25] leverage the log-probabilities of ground-truth answers as a reward signal, though they remain dependent on the availability of ground-truth trajectories.

In contrast to the above approaches, we propose to derive step-level rewards purely from the agent’s own internal representations, simultaneously addressing all the limitations they impose: no full-trajectory rollouts, no external LLM judges, no separately trained reward models, and no dependence on ground-truth answers during runtime.

2.3 Internal state probing for correctness prediction

A growing body of work demonstrates that LLM internal representations can be reliable indicators of model and correctness without external verification. Recent methods like CoE (Chain-of-Embedding) [22] explore training-free evaluation by observing changes in hidden state magnitudes and angles across layers. Furthermore, the entropy of attention heads are demonstrated to predict the correctness of LLM response [11], and Lookback ratio analysis [2] also identifies that attention to previous

context can signal hallucination. Despite their efficiency, these internal probes have primarily been validated in *clean-prefix* and *single-turn* settings. Our work addresses a critical gap: the failure of naive internal probes under *prefix contamination* in multi-turn scenarios. Our proposed PAIR reconciles this by adaptively combining hidden states with robust attention features to provide a reliable reward signal even in contaminated contexts.

3 Proposed Method

3.1 Motivation

Before presenting our method, we establish the empirical motivation: internal correctness probes fail systematically when the input prefix contains errors from earlier steps.

3.1.1 Problem Setup

We consider agentic tasks that require multi-step reasoning, repeated tool use, and environment interaction. Let $x \in \mathcal{X}$ be a task description sampled from a task distribution \mathcal{T} , and a task agent interacts with the environment to produce an execution trace τ and a final output \hat{y} . This process is denoted as:

$$x \rightarrow \tau \rightarrow \hat{y}. \quad (1)$$

The execution trace τ is defined as a sequence of states, actions, and observations:

$$\tau = (t_1, a_1, o_1, \dots, t_T, a_T, o_T) \quad (2)$$

where t_t is the agent’s thought (reasoning), a_t is the action taken (tool call), and o_t is the observation (tool output) received from the environment at step t . Each action a_t is generated by a policy π_θ conditioned on the prefix $p_t = (x, t_1, a_1, o_1, \dots, o_{t-1})$.

Prefix contamination. We say the prefix p_t is *contaminated* if one or more earlier thoughts t_j ($j < t$) or actions a_j ($j < t$) are erroneous—e.g., containing reasoning errors, tool misuse, observation misinterpretation, or reliance on wrong information. This is the typical condition during RL exploration, where the policy is imperfect and generates incorrect intermediate steps.

Evaluation setup. We construct matched clean/contaminated test pairs: for each reasoning trajectory, two versions of the prefix preceding the evaluation turn—one clean (all prior steps correct) and one contaminated (one or more prior steps replaced with erroneous alternatives)—are produced, with the evaluation turn held identical across the two so that any difference in probe accuracy isolates the effect of the prefix. We use Qwen-2.5-7B-Instruct [26] as our backbone and extract five feature types from the evaluation turn’s forward pass: three *hidden-state* features (Last-Token, Mean-Pooled, Multi-Layer) and two *attention-based* features (Attention, Hidden+Attn). All probes are linear, trained on the clean training split and evaluated on both clean and contaminated splits; we report AUROC. Detailed feature definitions, attention statistics, the probing protocol, and the AUROC metric are described in Appendix A.

Evaluation setup. We construct matched clean/contaminated test pairs: for each reasoning trajectory, we produce two versions of the prefix preceding the evaluation turn—one clean (all prior steps correct) and one contaminated (one or more prior steps replaced with erroneous alternatives). The detailed explanations of test pair construction is presented in Appendix A. The evaluation turn itself is identical across both versions, enabling controlled measurement of prefix effects on probe accuracy. We use Qwen-2.5-7B-Instruct [26] as our backbone model for all following experiments.

For each evaluation point in the test set, we have a triple (prefix, evaluation turn, correctness label), where the evaluation turn may be either correct or incorrect with respect to the gold task solution. Features are extracted by running the backbone forward through [prefix; evaluation turn] under teacher forcing—i.e., the evaluation turn is supplied as input rather than autoregressively generated—and reading out the hidden state and attention statistics at the evaluation turn’s tokens. The probing task is then a binary classification of the correctness label, and we report AUROC, the probability that the probe assigns a higher score to a correct evaluation turn than to an incorrect one.

We extract five feature types from the evaluation turn’s forward pass: *1) Last-Token*: the hidden state of the final token at the last layer (d_{model} dimensions). *2) Mean-Pooled*: the mean of all token hidden states within the evaluation turn at the last layer. *3) Multi-Layer*: concatenation of the last-token hidden states from the final 4 layers ($4 \times d_{\text{model}}$ dimensions). *4) Attention*: for each attention head in the last layer, we compute four statistics over the evaluation turn’s attention distribution: peak magnitude (`max_attn`), spread (`std_attn`), proportion attending to prefix tokens (`prefix_ratio`),

and proportion attending to own-turn tokens (`self_ratio`), yielding a $4 \times H$ -dimensional vector where H is the number of heads. 5) *Hidden+Attn*: concatenation of Last-Token and Attention features. All probes are StandardScaler + LogisticRegression (ℓ_2 penalty), trained on the clean training split and evaluated on both clean and contaminated test splits.

3.1.2 Key Findings

As shown in Figure 1, probes utilizing hidden-state exhibit significant AUROC drops when evaluated on contaminated prefixes compared to clean prefixes. However, attention probe shows smaller performance degradation under contamination. While it underperforms hidden-state probes on clean data, its relative robustness under contamination makes them valuable in mixed conditions. A naïve concatenation (Hidden+Attn) does not resolve this tension, as the hidden-state component can dominate and drag performance down under contamination.

This asymmetry is consistent with how LLM hidden states are shaped during pre-training: the next-token-prediction objective optimizes representations to capture *what is coherent with the prefix*, not what is objectively correct for the underlying task—the model receives no direct supervision for the latter. This view also aligns with prior probing studies, which show that internal probes tend to recover the model’s beliefs rather than external truth [1, 6].

Attention features, by contrast, capture *structural* behavior patterns—e.g., whether the model attends to task-relevant tokens versus merely following the corrupted narrative—which remain informative regardless of prefix quality. This robustness is consistent with the architectural role of attention: rather than encoding accumulated content, attention determines *where* information is routed at each step, and prior probing studies have successfully exploited this structural signal for hallucination detection and faithfulness analysis [2, 11].

Based on these observations, we hypothesize that the hidden state encodes *belief-consistency*—whether the current step is coherent with the accumulated prefix—rather than *grounded correctness*—whether the current step makes genuine progress toward the task goal. In other words, these two notions align under clean prefixes: a step that is coherent with a correct history is also likely correct. Under contaminated prefixes, on the other hand, they diverge: a step that perpetuates prior errors is belief-consistent but not grounded-correct, while a *repair step* that corrects a prior error is grounded-correct but belief-inconsistent.

3.1.3 Belief Consistency vs. Grounded Correctness

The preceding experiments establish that hidden-state probes degrade under prefix contamination while attention probes remain relatively robust. This raises a deeper mechanistic question: *do hidden-state probes track belief-consistency (coherence with the prefix) rather than grounded correctness (actual task utility)?* To answer this, we construct a controlled diagnostic dataset in which these two notions are deliberately placed in opposition.

Diagnostic construction. Each evaluation point is a triple (contaminated prefix, candidate turn, correctness label), where the prefix contains one or more erroneous prior steps. Within this dataset, coherence with the prefix and grounded correctness are deliberately *anti-correlated*.

Consistent-but-incorrect turn. A next turn that *fluently follows* the contaminated prefix—i.e., perpetuates the prior error in a contextually coherent way (e.g., calling the next tool that would be appropriate *if the wrong premise were true*). The turn is locally consistent with the prefix, but objectively wrong; the correctness label is *incorrect*.

Inconsistent-but-correct turn. A next turn that performs the *objectively correct* action for the underlying task, even though doing so contradicts the corrupted prefix (e.g., calling a different tool than the contaminated history would suggest). The turn appears incoherent with the prior context, but it is the correct next action; the correctness label is *correct*.

In contrast to the previous experiment, where the prefix could be either clean or contaminated, this diagnostic restricts to *contaminated prefixes only* paired with turns deliberately engineered to

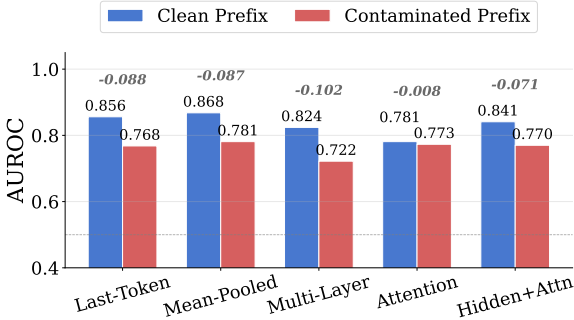


Figure 1: Comparison of AUROC degradation between hidden state probes and attention probes under clean vs. contaminated prefix settings.

be either strongly consistent-but-incorrect or strongly inconsistent-but-correct, so as to isolate the belief-consistency / grounded-correctness effect more directly. By construction, a reward signal that tracks *belief-consistency* will assign high scores to consistent-but-incorrect turns and low scores to inconsistent-but-correct repair turns—exactly the opposite of the gold labels. Its AUROC on this dataset will fall *at or below chance*. Conversely, a reward signal that tracks *grounded correctness* will correctly down-weight the locally fluent but wrong turn and up-weight the seemingly incoherent but correct repair turn, regardless of whether the candidate turn is coherent with the corrupted prefix; its AUROC will lie well above chance. Performance on this dataset is therefore a direct read-out of *which signal a probe is tracking*.

The results in Figure 2 confirm the mechanistic hypothesis: All three hidden-state probes score *at or below chance*, which means they consistently rank consistent-but-incorrect turns above inconsistent-but-correct turns. In an RL training loop, using such a probe as a reward would therefore actively *penalize* repair turns that overcome previous error and *reward* error-perpetuating turns. This failure is specific to hidden-state probes: the attention probe achieves AUROC well above chance, correctly identifying repair turns as more likely correct and error-perpetuating turns as more likely incorrect. Attention features therefore capture structural signals—whether the model attends to task-relevant information rather than merely following the corrupted narrative—that remain aligned with grounded correctness even when the prefix is contaminated.

It is worth noting that simply concatenating hidden-state and attention features (i.e., Hidden+Attn) does not resolve the conflict: the hidden-state component’s inverted signal cancels the attention component’s correct signal, yielding near-chance performance. This highlights the need for an adaptive feature integration strategy, rather than relying on simple feature concatenation. These findings provide direct mechanistic evidence for the design of PAIR: the hidden-state probe captures a meaningful but incomplete signal (belief-consistency), and the attention-based correction head compensates for exactly the cases where belief-consistency diverges from grounded correctness. Further analysis of sensitivity regarding to contamination distance is presented in Appendix B.

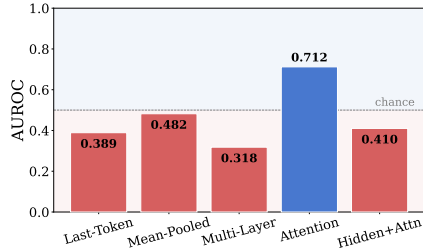


Figure 2: Comparison of hidden state and attention probes on the **adversarial diagnostic set**, where belief-consistency and grounded correctness are deliberately placed opposite.

3.2 Prefix-Aware Internal Reward Model (PAIR)

Our empirical findings expose a **belief-consistency bias** in hidden-state probes: since they encode coherence with the prefix rather than grounded correctness, using them directly as a reward in multi-turn RL would reward steps that perpetuate prior errors and penalize *repair turns* that contradict the contaminated history. Attention features, by contrast, remain aligned with grounded correctness even under contamination, but underperform hidden-state probes when the prefix is clean. A practical reward model must therefore preserve the strength of hidden-state probes on clean trajectories while exploiting attention features to correct the bias on contaminated ones.

To address this, we propose the **Prefix-Aware Internal Reward Model (PAIR)**. PAIR utilizes a two-stage architecture to decouple internal consistency from grounded utility:

Stage 1: Belief-consistency estimator. A pre-trained logistic regression probe maps hidden-state features to a belief-consistency score:

$$s_{bc} = \sigma(\mathbf{w}_1^\top \mathbf{h} + b_1), \quad (3)$$

where $\mathbf{h} \in \mathbb{R}^{d_{\text{model}}}$ is the last-token hidden state, (\mathbf{w}_1, b_1) are the learned weights of the logistic regression probe, and σ is the sigmoid function. This probe is trained on clean data and then *frozen*—it captures what standard probes do well.

Stage 2: Attention-based correction. A second logistic regression model takes the attention features concatenated with s_{bc} and predicts the final correctness score:

$$s_{\text{final}} = \sigma(\mathbf{w}_2^\top [\mathbf{a}; s_{bc}] + b_2), \quad (4)$$

where $\mathbf{a} \in \mathbb{R}^{d_{\text{attn}}}$ is the multi-layer attention feature vector ($4 \text{ statistics} \times H \text{ heads} \times L \text{ layers}$), and (\mathbf{w}_2, b_2) are the learned weights of the correction head. The detailed ablation study of each feature is presented in Appendix D. This correction head is trained on a mixture of clean and contaminated

Table 2: Step-level correctness prediction performance on GTA and ToolBench. Each evaluation point is a single (prefix, evaluation turn) pair labelled correct or incorrect, not a trajectory-level outcome. **AUROC** (higher is better) and **ECE** (lower is better) are reported for each method. All AUROC and ECE values are reported as mean over 3 random seeds (42, 43, 44).

Dataset	Metric	Last-token	Mean-Pooled	Multi-layer	Attention	Hidden + Attn
GTA	AUROC	0.8967 \pm 0.012	0.8851 \pm 0.014	0.9082 \pm 0.010	0.8709 \pm 0.015	0.8978 \pm 0.013
	ECE	0.1294 \pm 0.018	0.1521 \pm 0.020	0.1342 \pm 0.017	0.0954\pm0.014	0.1378 \pm 0.018
ToolBench	AUROC	0.7654 \pm 0.008	0.7372 \pm 0.009	0.7821 \pm 0.007	0.6847 \pm 0.011	0.7598 \pm 0.008
	ECE	0.2562 \pm 0.014	0.2871 \pm 0.016	0.2476 \pm 0.013	0.1998 \pm 0.011	0.2683 \pm 0.015
Dataset	Metric	Multi-Attn	Lookback Lens[2]	Head Entropy[11]	CoE-C[22]	Ours (PAIR)
GTA	AUROC	0.9034 \pm 0.011	0.8745 \pm 0.014	0.8821 \pm 0.013	0.7491 \pm 0.022	0.9217\pm0.009
	ECE	0.1356 \pm 0.018	0.1182 \pm 0.015	0.1432 \pm 0.019	–	0.1198 \pm 0.014
ToolBench	AUROC	0.7765 \pm 0.007	0.7295 \pm 0.010	0.7561 \pm 0.009	0.5953 \pm 0.013	0.8129\pm0.006
	ECE	0.1961 \pm 0.011	0.1685\pm0.010	0.2329 \pm 0.013	–	0.2236 \pm 0.012

trajectories with the frozen Stage 1 score s_{bc} as one of its inputs—it thereby learns to leave s_{bc} alone on clean prefixes and to correct it where belief-consistency diverges from grounded correctness.

Design rationale. Under clean prefixes, s_{bc} already approximates grounded correctness accurately, so the optimal Stage 2 output is $s_{final} \approx s_{bc}$. In contrast, the attention features detect structural anomalies under contaminated prefixes and produce $s_{final} \approx s_{bc}$ that corrects the belief-consistency estimate toward grounded correctness. This design *structurally* ensures that clean-prefix performance is preserved. The detailed training and inference process is presented in Appendix C.

3.3 Comparison with Baselines

We evaluate PAIR against a comprehensive set of internal probing baselines spanning three categories: 1) hidden state probes, 2) attention probes, and 3) unsupervised internal signal methods.

1) Hidden state probes. *Last-Token* trains a linear probe on the hidden state of the final generated token at the last layer. *Mean-Pooled* averages hidden states across all tokens in the generated response before probing. *Multi-Layer* concatenates hidden states from multiple layers of the last token, capturing representations at different levels of abstraction.

2) Attention probes. *Attention* extracts summary statistics from attention weight of last layer—including maximum attention, standard deviation, prefix attention ratio, and self-attention ratio—and trains a linear probe on these features. *Multi-Attn* concatenates same statistics with *Attention* from all layers. *Hidden + Attn* concatenates the Multi-Layer hidden state features with the attention features and trains a single joint probe.

3) Unsupervised internal signal methods. *Lookback Lens* [2] detects hallucination by measuring the ratio of attention directed toward the context versus newly generated tokens. *Head Entropy* [11] uses the entropy of attention head distributions as an indicator of model uncertainty, where higher entropy suggests lower confidence in the generated content. *CoE-C* [22] leverage Chain-of-Embedding trajectories from the hidden states on real-space and complex-space, respectively, to predict the correctness of the LLM responses.

Results. Table 2 reports AUROC and Expected Calibration Error (ECE) on GTA and ToolBench. AUROC measures whether the probe ranks correct turns above incorrect ones, while ECE measures the gap between the probe’s predicted probability and the empirical correctness frequency. ECE matters in our setting because the probe’s output is used as a continuous reward in GRPO, where overconfident or miscalibrated scores compress the within-group reward variance and weaken the resulting advantage signal.

PAIR achieves the highest AUROC across both datasets, outperforming all individual probes as well as unsupervised baselines. While PAIR does not achieve the lowest ECE in all cases, its calibration remains comparable to other probing methods and substantially better than the hidden state probes, which tend to produce overconfident predictions. These results establish that PAIR provides a reliable correctness signal at the step level—a prerequisite for its deployment as a dense reward model in GRPO training. Unlike LLM-as-judge approaches that incur additional inference costs per step, PAIR operates at probe-level computational overhead, making it practical for online RL settings where reward must be computed for every step of every rollout.

4 Downstream RL Experiments

Having established that PAIR provides reliable step-level correctness signals even under prefix contamination (Section 3), we now evaluate whether these signals translate into effective reward models for multi-turn agent training via GRPO.

4.1 Experimental Setup

Datasets. We evaluate on two multi-step agent benchmarks that represent realistic agentic settings—as opposed to the search-augmented QA benchmarks (e.g., HotpotQA, NQ) used by prior internal reward methods. In multi-step tool use tasks, there is no single gold answer string; multiple valid action sequences can achieve the same outcome, and errors propagate through environment state rather than merely resulting in missing information. Specifically, **GTA** (General Tool Agents) [19] is a benchmark containing 229 samples where agents use diverse real-world APIs. Trajectories average 2–8 turns and require multi-step tool composition. **ToolBench** [13] is a dataset covering 16,000+ RapidAPI tools. We stratified 1,000 samples (minimum 3 turns) from the full dataset. Agents follow a Thought/Action/Action-Input/Observation loop. The detailed evaluation protocol is described in Appendix H.

Model. We use **Qwen2.5-7B-Instruct** [26] as the policy model for all GRPO experiments. Internal representations for PAIR are extracted from the same model being trained; no separate reward model is required. The detailed configuration for training is presented in Appendix G.

Reward baselines. We compare PAIR against reward methods spanning five categories:

- **Outcome-only:** Standard GRPO with a sparse binary reward assigned only at trajectory completion.
- **External reward:** *LLM Judge* uses GPT-4o-mini to evaluate each step’s quality on a 1–10 scale. Input prompt for LLM Judge is presented in Figure 10.
- **Tree-based:** *AT²PO* [33] performs tree-structured rollouts with entropy-weighted reward back-propagation. *Tree-GRPO* [5] uses intra- and inter-tree advantage normalization.
- **Internal probes:** We apply each probing method from Section 3.3 directly as a step-level reward model, using the predicted correctness probability as the per-step reward. This includes hidden-state probes (*Last-Token*, *Mean-Pooled*, *Multi-Layer*), attention probes (*Attention*, *Hidden+Attn*, *Multi-Attn*), and unsupervised methods (*Lookback Ratio* [2], *Head Entropy* [11], *CoE* [22]).
- **Intrinsic rewards:** *IGPO* [17] computes information gain via teacher-forced gold log-probabilities. *TIPS* [25] uses potential-based reward shaping with a lagged teacher.

Our baselines fall into two structurally different classes. **(I) Reward sources for vanilla GRPO** share the same training pipeline and differ only in the per-step reward signal: PAIR, Outcome-only, LLM-as-a-judge, and all internal-probe baselines. **(II) Specialized RL training algorithms** change the optimization scheme itself (*Tree-GRPO*, *AT²PO*, *IGPO*, and *TIPS*). Comparing across both classes tests whether PAIR—a reward source—can match methods that change the RL algorithm itself.

PAIR based Momentum Reward Integration. At each step t of a rollout, we extract the hidden state \mathbf{h}_t and attention features \mathbf{a}_t from the policy’s forward pass and compute the PAIR score $s_{final,t}$ via Eq. 4. Although $s_{final,t}$ can in principle be used directly as a step-level reward, doing so in GRPO leads to weak group-relative advantages: trajectories sharing a prompt receive similar absolute scores, so the within-group variance that GRPO relies on for credit assignment shrinks rapidly during training. We therefore use PAIR’s score as the input to a *momentum-based* reward that explicitly contrasts the current step against the trajectory’s running mean, recovering the variance needed for advantage estimation. The detailed description of reward design is presented in Appendix E.

4.2 Experimental Results

Table 3 reports success rate for all 16 methods, trained and evaluated separately on each of the two agent benchmarks (GTA and ToolBench). PAIR achieves the best result on both GTA and ToolBench, outperforming the second-best baseline, LLM-as-a-judge.

Two observations follow from this pattern. First, PAIR is the *only* method that ranks at the top on both datasets simultaneously, while every other approach is well-matched to one benchmark but mismatched to the other. *Rollout-based methods* (*Tree-GRPO*, *AT²PO*) compute advantages from K sibling rollouts whose reliability depends on each benchmark’s branching factor and trajectory length, so a fixed K may suffice on one benchmark while producing noisy advantages on the other;

Table 3: Overall performance comparison across all methods on GTA and ToolBench. Values are reported as mean \pm std over 3 random seeds (42, 43, 44).

Dataset	Outcome	LLM-as-a-judge	Last-token	Multi-layer
GTA	0.1851 \pm 0.055	0.2387 \pm 0.042	0.1372 \pm 0.060	0.1789 \pm 0.058
ToolBench	0.3878 \pm 0.035	0.4203 \pm 0.028	0.3837 \pm 0.038	0.3856 \pm 0.037
Dataset	Mean-pooled	Attention	Hidden+Attn	Multi-Attn
GTA	0.1798 \pm 0.060	0.2154 \pm 0.048	0.1432 \pm 0.062	0.2218 \pm 0.046
ToolBench	0.3917 \pm 0.037	0.3471 \pm 0.030	0.3784 \pm 0.038	0.3614 \pm 0.030
Dataset	Lookback-ratio [2]	Head-entropy [11]	CoE-C [22]	IGPO [17]
GTA	0.1812 \pm 0.050	0.1989 \pm 0.048	0.1721 \pm 0.055	0.2005 \pm 0.052
ToolBench	0.3934 \pm 0.030	0.3868 \pm 0.030	0.4034 \pm 0.034	0.3952 \pm 0.032
Dataset	TIPS [25]	Tree-GRPO [5]	AT ² PO [33]	PAIR
GTA	0.1856 \pm 0.058	0.1934 \pm 0.058	0.1865 \pm 0.055	0.2489\pm0.042
ToolBench	0.3483 \pm 0.035	0.3935 \pm 0.035	0.3812 \pm 0.034	0.4498\pm0.025

intrinsic methods (IGPO, TIPS) score steps by the model’s log-probability of the gold answer, which systematically under-rewards correct early steps in long trajectories—the gold answer is still many tokens away, so its log-probability remains low even when the step is on the right path; *LLM-as-a-judge* relies on a single judge prompt’s fit to each benchmark’s task structure—a prompt tuned for one task style may produce uninformative or biased scores on the other; and single-signal *internal probes* (Last-token, Mean-pooled, Multi-layer, Attention, CoE, Lookback, Head-entropy) commit to one feature type whose discriminative power depends on each benchmark’s error distribution—e.g., hidden-state features tend to be most informative when reasoning errors dominate, attention features when tool-misuse errors dominate. PAIR is the only design without such a fixed assumption: it depends on neither rollout structure, gold answers, nor external judges, and *adaptively* combines two complementary internal signals (hidden state and attention) rather than committing to either alone.

Second, the only baseline that competes with PAIR on either dataset is LLM-as-a-judge, and its competitiveness comes at a cost that is fundamentally incompatible with the use case we target. LLM-as-a-judge requires an external LLM call *per step* of the agent’s trajectory to obtain a reward signal: as a step-level reward source for online GRPO training, this incurs hundreds to thousands of additional API calls per training episode, multiplied by the number of episodes per training run. The resulting wall-clock latency and monetary cost make it effectively unusable as a dense step-level reward at any non-trivial training scale, regardless of its accuracy. PAIR, in contrast, runs a single forward pass of the agent’s own model—reusing the activations the agent has already computed—and produces step-level rewards at probe-level marginal cost (logistic regression over a vector of pre-existing features). Further analysis for computing cost is presented in Appendix F.

Combining the two observations, PAIR offers the best practical operating point in the comparison: it is the strongest method on ToolBench by a clear margin, statistically indistinguishable from the strongest method on GTA, and the only top-ranked method that does not require external model calls, ground-truth supervision at inference, or full-trajectory rollouts.

Effect of Momentum-based reward. The probe output $s_{final,t}$ produced by PAIR’s two-stage architecture can be used directly as a step-level reward in GRPO, without any further transformation. It already yields a competitive operating point: as Figure 3 shows, the vanilla PAIR—which uses $s_{final,t}$ as the per-step reward attains 0.230 on GTA and 0.415 on ToolBench, on par with the strongest non-PAIR baselines in Table 3. The probe alone is therefore already a usable replacement for external or rollout-based reward signals, validating the probe-as-reward design at the level of the underlying correctness predictor. The momentum-based variant used in our main results goes one step further by adding an explicit contrast between each step’s score and the trajectory’s running mean. This reward-shaping step yields a consistent improvement on top of the vanilla variant. The takeaway is that PAIR’s

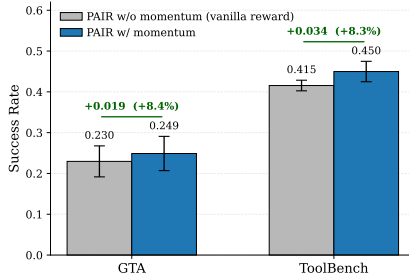


Figure 3: Effect of the momentum reward. PAIR with the momentum-based reward outperforms the vanilla by $\approx 8\%$ on both GTA and ToolBench.

effectiveness does not rest solely on the probe being a good correctness predictor—*how* the probe output is integrated into the GRPO objective also matters, and the momentum formulation extracts measurably more learning signal from the same underlying probe. More detailed hyperparameter analysis is described in Appendix I.

4.3 Cross-domain Transfer

To test whether PAIR’s signal is anchored to a transferable property of the agent’s computation rather than to dataset-specific surface features, we additionally evaluate cross-domain transfer: all reward models are trained on GTA and applied, without any adaptation, to HotpotQA—a multi-hop reasoning benchmark that shares the multi-step structure of agentic tasks but differs substantially in distribution. As shown in Figure 4, PAIR ranks first among all 16 methods, and three patterns in the ranking corroborate its design rationale.

First, attention-based methods (Head-entropy, Attention, Lookback-ratio) occupy the top of the table while every hidden-state-only probe falls to the middle. Attention patterns reflect structural aspects of the model’s computation—properties of the underlying transformer mechanism rather than of task content—and therefore transfer more gracefully than hidden states, which encode semantic information of the training distribution. This extends the asymmetry observed under *prefix contamination* (Section 3.1.2) to *distributional shift*.

Second, naive concatenation of hidden-state and attention features (Hidden+Attn) underperforms standalone Attention: the unreliable hidden-state component drags down the more robust attention signal under domain shift. PAIR instead places hidden state in a fixed residual base and lets the attention head learn an additive correction in logit space, structurally protecting the attention signal—and ranks above both. The same two information sources thus yield a loss under concatenation but a gain under PAIR, isolating the value of the architectural decoupling itself.

Third, methods that incur rollout, external-model, or ground-truth costs occupy the bottom of the table: rollout-based methods (Tree-GRPO, AT²PO) inherit high training-time variance from K -sample sibling estimates that compounds under domain shift; ground-truth-dependent methods (IGPO, TIPS) shape policies around GTA’s gold-answer format, mismatching HotpotQA’s short-span answers; and LLM-as-a-judge inherits judge biases tuned for GTA-style tasks while remaining prohibitive at training scale via API costs. Across all comparisons, PAIR is the only method that simultaneously achieves the highest accuracy, operates without ground-truth at inference, requires no rollouts or external model calls, and transfers across domains without re-training—directly addressing the four limitations identified in the introduction.

5 Conclusion

We have identified a critical failure mode of internal correctness probes in multi-step agent settings: prefix contamination causes hidden-state probes to track belief-consistency rather than grounded correctness, producing reward signals that actively discourage error correction. Through systematic analysis, we showed that attention features provide a complementary, more robust signal that captures structural behavior patterns. Building on these findings, we proposed the PAIR, a two-stage reward architecture that freezes a hidden-state probe as a belief-consistency estimator and applies a lightweight attention-based correction to bridge the gap to grounded correctness. PAIR preserves strong performance under clean conditions while recovering robustness under contamination, all at probe-level inference cost. By enabling dense, step-level reward signals without external model calls, runtime ground-truth dependencies, or separate reward model training, PAIR makes probe-based reward practical for multi-step agent RL training. We believe this work opens a promising direction at the intersection of internal state analysis and reinforcement learning for LLM agents.

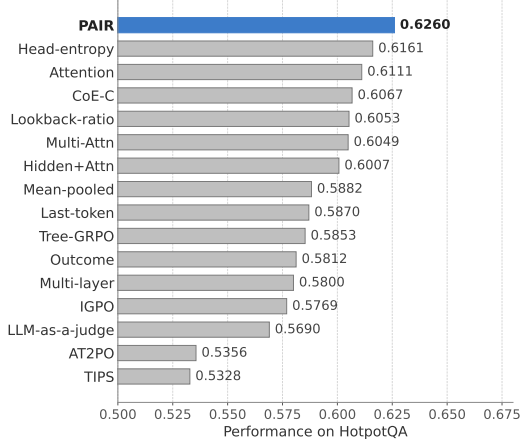


Figure 4: Transfer performance on HotpotQA. Each method is trained on GTA and evaluated on HotpotQA without further fine-tuning. PAIR achieves the best result among all 16 methods.

References

- [1] Collin Burns, Haotian Ye, Dan Klein, and Jacob Steinhardt. Discovering latent knowledge in language models without supervision. *arXiv preprint arXiv:2212.03827*, 2022.
- [2] Yung-Sung Chuang, Linlu Qiu, Cheng-Yu Hsieh, Ranjay Krishna, Yoon Kim, and James Glass. Lookback lens: Detecting and mitigating contextual hallucinations in large language models using only attention maps. In *Proceedings of the 2024 Conference on Empirical Methods in Natural Language Processing*, pages 1419–1436, 2024.
- [3] Jiawei Gu, Xuhui Jiang, Zhichao Shi, Hexiang Tan, Xuehao Zhai, Chengjin Xu, Wei Li, Yinghan Shen, Shengjie Ma, Honghao Liu, et al. A survey on llm-as-a-judge. *The Innovation*, 2024.
- [4] Daya Guo, Dejian Yang, Haowei Zhang, Junxiao Song, Peiyi Wang, Qihao Zhu, Runxin Xu, Ruoyu Zhang, Shirong Ma, Xiao Bi, et al. Deepseek-r1: Incentivizing reasoning capability in llms via reinforcement learning. *arXiv preprint arXiv:2501.12948*, 2025.
- [5] Yuxiang Ji, Ziyu Ma, Yong Wang, Guanhua Chen, Xiangxiang Chu, and Liaoni Wu. Tree search for llm agent reinforcement learning. *arXiv preprint arXiv:2509.21240*, 2025.
- [6] Saurav Kadavath, Tom Conerly, Amanda Askell, Tom Henighan, Dawn Drain, Ethan Perez, Nicholas Schiefer, Zac Hatfield-Dodds, Nova DasSarma, Eli Tran-Johnson, et al. Language models (mostly) know what they know. *arXiv preprint arXiv:2207.05221*, 2022.
- [7] Wonjoong Kim, Sangwu Park, Yeonjun In, Sein Kim, Dongha Lee, and Chanyoung Park. Beyond the final answer: Evaluating the reasoning trajectories of tool-augmented agents. *arXiv preprint arXiv:2510.02837*, 2025.
- [8] Hunter Lightman, Vineet Kosaraju, Yuri Burda, Harrison Edwards, Bowen Baker, Teddy Lee, Jan Leike, John Schulman, Ilya Sutskever, and Karl Cobbe. Let’s verify step by step. In *The twelfth international conference on learning representations*, 2023.
- [9] Zichen Liu, Changyu Chen, Wenjun Li, Penghui Qi, Tianyu Pang, Chao Du, Wee Sun Lee, and Min Lin. Understanding r1-zero-like training: A critical perspective. *arXiv preprint arXiv:2503.20783*, 2025.
- [10] Qianli Ma, Haotian Zhou, Tingkai Liu, Jianbo Yuan, Pengfei Liu, Yang You, and Hongxia Yang. Let’s reward step by step: Step-level reward model as the navigators for reasoning. *arXiv preprint arXiv:2310.10080*, 2023.
- [11] Sophie Ostmeier, Brian Axelrod, Maya Varma, Asad Aali, Yabin Zhang, Magdalini Paschali, Sanmi Koyejo, Curtis Langlotz, and Akshay Chaudhari. Attention head entropy of llms predicts answer correctness. *arXiv preprint arXiv:2602.13699*, 2026.
- [12] Long Ouyang, Jeffrey Wu, Xu Jiang, Diogo Almeida, Carroll Wainwright, Pamela Mishkin, Chong Zhang, Sandhini Agarwal, Katarina Slama, Alex Ray, et al. Training language models to follow instructions with human feedback. *Advances in neural information processing systems*, 35:27730–27744, 2022.
- [13] Yujia Qin, Shihao Liang, Yining Ye, Kunlun Zhu, Lan Yan, Yaxi Lu, Yankai Lin, Xin Cong, Xiangru Tang, Bill Qian, et al. Toolllm: Facilitating large language models to master 16000+ real-world apis. *arXiv preprint arXiv:2307.16789*, 2023.
- [14] John Schulman, Filip Wolski, Prafulla Dhariwal, Alec Radford, and Oleg Klimov. Proximal policy optimization algorithms. *arXiv preprint arXiv:1707.06347*, 2017.
- [15] Zhihong Shao, Peiyi Wang, Qihao Zhu, Runxin Xu, Junxiao Song, Xiao Bi, Haowei Zhang, Mingchuan Zhang, YK Li, Yang Wu, et al. Deepseekmath: Pushing the limits of mathematical reasoning in open language models. *arXiv preprint arXiv:2402.03300*, 2024.
- [16] Nisan Stiennon, Long Ouyang, Jeffrey Wu, Daniel Ziegler, Ryan Lowe, Chelsea Voss, Alec Radford, Dario Amodei, and Paul F Christiano. Learning to summarize with human feedback. *Advances in neural information processing systems*, 33:3008–3021, 2020.
- [17] Guoqing Wang, Sunhao Dai, Guangze Ye, Zeyu Gan, Wei Yao, Yong Deng, Xiaofeng Wu, and Zhenzhe Ying. Information gain-based policy optimization: A simple and effective approach for multi-turn llm agents. *arXiv preprint arXiv:2510.14967*, 2025.

- [18] Hanlin Wang, Chak Tou Leong, Jiashuo Wang, Jian Wang, and Wenjie Li. Spa-rl: Reinforcing llm agents via stepwise progress attribution. *arXiv preprint arXiv:2505.20732*, 2025.
- [19] Jize Wang, Zerun Ma, Yining Li, Songyang Zhang, Cailian Chen, Kai Chen, and Xinyi Le. Gta: a benchmark for general tool agents. *Advances in Neural Information Processing Systems*, 37:75749–75790, 2024.
- [20] Peiyi Wang, Lei Li, Zhihong Shao, RX Xu, Damai Dai, Yifei Li, Deli Chen, Yu Wu, and Zhifang Sui. Math-shepherd: Verify and reinforce llms step-by-step without human annotations, 2024. URL <https://arxiv.org/abs/2312.08935>, 2(3), 2024.
- [21] Weiyun Wang, Zhangwei Gao, Lianjie Chen, Zhe Chen, Jinguo Zhu, Xiangyu Zhao, Yangzhou Liu, Yue Cao, Shenglong Ye, Xizhou Zhu, et al. Visualprm: An effective process reward model for multimodal reasoning. *arXiv preprint arXiv:2503.10291*, 2025.
- [22] Yiming Wang, Pei Zhang, Baosong Yang, Derek F Wong, and Rui Wang. Latent space chain-of-embedding enables output-free llm self-evaluation. *arXiv preprint arXiv:2410.13640*, 2024.
- [23] Quan Wei, Siliang Zeng, Chenliang Li, William Brown, Oana Frunza, Wei Deng, Anderson Schneider, Yuriy Nevmyvaka, Yang Katie Zhao, Alfredo Garcia, et al. Reinforcing multi-turn reasoning in llm agents via turn-level reward design. *arXiv preprint arXiv:2505.11821*, 2025.
- [24] Zhiheng Xi, Chenyang Liao, Guanyu Li, Yajie Yang, Wenxiang Chen, Zhihao Zhang, Binghai Wang, Senjie Jin, Yuhao Zhou, Jian Guan, et al. Agentprm: Process reward models for llm agents via step-wise promise and progress. *arXiv preprint arXiv:2511.08325*, 2025.
- [25] Yutao Xie, Nathaniel Thomas, Nicklas Hansen, Yang Fu, Li Erran Li, and Xiaolong Wang. Tips: Turn-level information-potential reward shaping for search-augmented llms. *arXiv preprint arXiv:2603.22293*, 2026.
- [26] An Yang, Baosong Yang, Beichen Zhang, Binyuan Hui, Bo Zheng, Bowen Yu, et al. Qwen2.5 technical report. *arXiv preprint arXiv:2412.15115*, 2024.
- [27] Zhangyue Yin, Qiushi Sun, Zhiyuan Zeng, Qinyuan Cheng, Xipeng Qiu, and Xuan-Jing Huang. Dynamic and generalizable process reward modeling. In *Proceedings of the 63rd Annual Meeting of the Association for Computational Linguistics (Volume 1: Long Papers)*, pages 4203–4233, 2025.
- [28] Hanning Zhang, Pengcheng Wang, Shizhe Diao, Yong Lin, Rui Pan, Hanze Dong, Dylan Zhang, Pavlo Molchanov, and Tong Zhang. Entropy-regularized process reward model. *arXiv preprint arXiv:2412.11006*, 2024.
- [29] Xiaoying Zhang, Yipeng Zhang, Hao Sun, Kaituo Feng, Chaochao Lu, Chao Yang, and Helen Meng. Critique-grpo: Advancing llm reasoning with natural language and numerical feedback. *arXiv preprint arXiv:2506.03106*, 2025.
- [30] Zhenru Zhang, Chujie Zheng, Yangzhen Wu, Beichen Zhang, Runji Lin, Bowen Yu, Dayiheng Liu, Jingren Zhou, and Junyang Lin. The lessons of developing process reward models in mathematical reasoning. In *Findings of the Association for Computational Linguistics: ACL 2025*, pages 10495–10516, 2025.
- [31] Hongyi Zhou, Kai Ye, Erhan Xu, Jin Zhu, Ying Yang, Shijin Gong, and Chengchun Shi. Demystifying group relative policy optimization: Its policy gradient is a u-statistic. *arXiv preprint arXiv:2603.01162*, 2026.
- [32] Yifei Zhou, Song Jiang, Yuandong Tian, Jason Weston, Sergey Levine, Sainbayar Sukhbaatar, and Xian Li. Sweet-rl: Training multi-turn llm agents on collaborative reasoning tasks. *arXiv preprint arXiv:2503.15478*, 2025.
- [33] Zefang Zong, Dingwei Chen, Yang Li, Qi Yi, Bo Zhou, Chengming Li, Bo Qian, Peng Chen, and Jie Jiang. At²po: Agentic turn-based policy optimization via tree search. *arXiv preprint arXiv:2601.04767*, 2026.

Supplementary Material for
PAIR: Prefix-Aware Internal Reward Model for
Multi-Turn Agent Optimization

A	Data Contamination for Motivation Experience	14
A.1	Source Trajectories and Splits	14
A.2	Contamination Types	14
A.3	Diagnostic Pairs for the Belief-Consistency Hypothesis	14
A.4	Contamination Procedure	15
B	Sensitivity Analysis Regarding to Contamination Distance	15
C	Training & Inference of PAIR	16
C.1	training	16
C.2	Inference as Step-Level Reward	16
D	Ablation Study for Attention Statistics	17
E	Detailed Reward Design with PAIR	17
F	Complexity Analysis	18
G	GRPO Training Configuration	19
H	Detailed Evaluation Process	20
I	Hyperparameter Analysis	21
J	Limitation and Future Work	22
K	Prompts	23

A Data Contamination for Motivation Experience

We present details of the construction of the matched clean / contaminated trajectory pairs used in the motivation experiments (Section 3.1.2) and as the offline training corpus for PAIR (Section 4). We describe the source data (§A.1), the four contamination types and their dataset-specific adaptations (§A.2), the construction of the diagnostic *belief-consistency* and *grounded-correctness* turns used in Figure 2 (§A.3), and the contamination procedure (§A.4). The full prompts used to drive contamination with GPT-4o-mini are reproduced in Figure 8 and 9.

A.1 Source Trajectories and Splits

We construct contaminated trajectories from two multi-turn agent benchmarks: **GTA** [19] and **ToolBench** [13]. Both follow the canonical agentic format

$$\tau = (x, t_1, a_1, o_1, \dots, t_T, a_T, o_T),$$

where x is the task description, and each step consists of a thought t_i , an action / tool call a_i , and an observation o_i returned by the environment. We apply two filters to obtain trajectories suitable for contamination: (i) at least *three* assistant turns (so that contamination can be applied to a non-evaluation turn while leaving at least one upstream turn intact); and (ii) trajectory length ≤ 8 turns, which covers $> 96\%$ of episodes in both datasets and avoids context-window blow-up under our backbone (Qwen2.5-7B-Instruct, 4,096-token context).

For each dataset we apply an 80:20 stratified train / test split with a fixed seed (42). For ToolBench we additionally subsample 1,000 episodes from the 48,454-episode source release using stratified sampling on trajectory length, yielding the final episode counts in Table 4.

Table 4: Episode counts in each split before and after contamination filtering. $clean_{tr}$ / $clean_{te}$ are the original splits used as anchors; $contam_{tr}$ / $contam_{te}$ are the matched contaminated versions where exactly one prior assistant turn has been replaced with an erroneous alternative.

Dataset	Source episodes	$clean_{tr}$	$contam_{tr}$	$clean_{te}$	$contam_{te}$
GTA	229	183	183	46	46
ToolBench	1,000 (sampled)	800	800	200	200

A.2 Contamination Types

We instantiate four canonical failure modes observed in deployed agentic systems. Each type targets a specific component of the multi-step trajectory (reasoning, action, observation handling, or working memory), giving full coverage of the ways an upstream turn can damage downstream credit assignment.

- **Reasoning error.** The chosen assistant thought t_j is rewritten to contain a logically flawed inference that nonetheless appears fluent and contextually coherent. The corrupted thought is one that a reasonable but mistaken policy could plausibly produce.
- **Tool misuse.** The chosen action a_j is rewritten to invoke an inappropriate tool, supply a malformed argument, or call the right tool with semantically wrong parameters.
- **Observation misinterpretation.** The chosen thought t_j is rewritten so that it reaches a conclusion that is inconsistent with the immediately preceding observation o_{j-1} — for example, claiming an API call succeeded when its response indicates failure, or extracting the wrong field from a tool output.
- **Stale memory.** The chosen turn is rewritten to rely on information from earlier in the trajectory in a way that contradicts later evidence — for example, persisting an outdated value as if it were current.

A.3 Diagnostic Pairs for the Belief-Consistency Hypothesis

The motivation experiment of Figure 2 requires turns where *belief-consistency* and *grounded correctness* are deliberately placed in opposition. We construct two complementary turn types for each base trajectory.

Belief-consistency turn (looks right, is wrong). Given a *clean* prefix, we generate a next assistant turn that is fluent and locally coherent with the conversation history but does not advance task completion: a redundant retrieval, an unnecessary clarification, or a syntactically valid tool call that retrieves task-irrelevant information. The turn is locally indistinguishable from a normal continuation but contributes nothing to the gold solution.

Grounded-correctness turn (looks wrong, is right). Given a *contaminated* prefix, we generate a next assistant turn that performs the objectively correct next action, regardless of whether it is locally coherent with the contaminated history. Concretely, the generator is conditioned on (i) the original *clean* task description, (ii) the contaminated prefix, and (iii) the gold next action, and is instructed to produce the gold action even if it contradicts the immediately preceding (contaminated) turn. These are the analogue of *repair turns*: turns that detect the prior error and override it.

The resulting maximally adversarial pair — a *looks-right-but-wrong* turn after a clean prefix and a *looks-wrong-but-right* turn after a contaminated prefix — is what the probes in Figure 2 are scored on.

A.4 Contamination Procedure

For each clean trajectory $\tau = (x, t_1, a_1, o_1, \dots, t_T, a_T, o_T)$ with $T \geq 3$ assistant turns, we designate the *last* assistant turn (t_T, a_T) as the *evaluation turn* and the prefix $p_T = (x, t_1, a_1, o_1, \dots, o_{T-1})$ as the contamination target. The procedure is as follows:

1. **Pick a contamination target.** Sample one assistant turn $j \in \{1, \dots, T-1\}$ uniformly at random.
2. **Pick a contamination type.** Sample a contamination type from the set of types compatible with the chosen turn (e.g., *tool_misuse* requires that the chosen turn contain a tool call; cf. Table 5).
3. **Generate the corrupted turn.** Issue a single GPT-4o-mini call with the type-specific system prompt (Figure 8 and Figure 9) and the relevant turn context, instructing the model to rewrite the chosen turn as a plausible-looking but objectively incorrect version of the original.
4. **Preserve downstream.** Replace turn j in the trajectory with the corrupted version. *Do not modify any other turn*, including all subsequent observations and the evaluation turn (t_T, a_T) . This preserves matched-pair semantics: each $(\tau^{\text{clean}}, \tau^{\text{contam}})$ pair differs only in turn j , and the evaluation turn over which we measure probe accuracy is identical across the two.
5. **Log metadata.** For every contaminated episode we record the contamination type, the index j of the corrupted turn, the original turn content, and the GPT-4o-mini response, enabling downstream auditing and validation.

Table 5: Compatibility of contamination types with trajectory structures, and the empirical distribution of types over the union of contam_{r} and contam_{e} for each dataset. *Reasoning* is always applicable; the remaining types are gated on the structure of the chosen turn, so their empirical frequencies follow the structure of each dataset.

Type	Compatible turns	GTA %	ToolBench %
reasoning_error	all assistant turns	25.7	26.1
tool_misuse	turns with a tool call	26.4	25.8
observation_misinterpretation	turns preceded by a tool observation	24.5	25.3
stale_memory	trajectories with ≥ 3 asst. turns	23.4	22.8

The *evaluation turn* is held identical across the two versions of the trajectory. Any difference in probe AUROC between τ^{clean} and τ^{contam} can therefore be attributed to the prefix alone, not to differences in the step being scored. This matched-pair design is what makes the contamination effect causally identifiable in Figure 1.

B Sensitivity Analysis Regarding to Contamination Distance

We further examine how each probe’s accuracy depends on the temporal distance d between the contaminated turn and the evaluation turn ($d = 1$: the error is the immediately preceding turn; larger d : the error sits deeper in the prefix). Figure 5 reports per-probe accuracy stratified by d on both benchmarks.

Two patterns are visible across the two benchmarks. **First, all probes degrade as the contaminated turn moves further from the evaluation turn.** Long-range contaminations are harder to recover

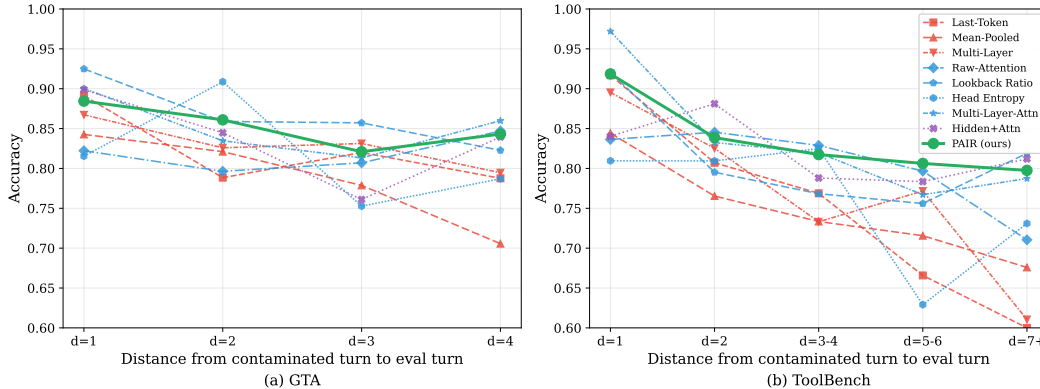


Figure 5: Correctness prediction performance of linear probing models regarding to different contamination distances.

from the evaluation turn’s local representations alone: by the time the evaluation turn is processed, the model’s belief state has had several intervening (correct) turns to re-stabilize around the corrupted prefix, so the local features of the evaluation turn carry less direct evidence of the distant error. The effect is mild on GTA, whose trajectories are short ($d \leq 4$), but is pronounced on ToolBench, where d extends to 7+ and accuracy spans roughly 0.60 to 0.95 across the range.

Second, hidden-state probes degrade more steeply with distance than attention probes. On ToolBench, the three hidden-state probes (Last-Token, Mean-Pooled, Multi-Layer) start from ≈ 0.85 – 0.90 at $d = 1$ and drop to 0.60 – 0.68 at $d = 7+$, whereas attention-based probes (Raw-Attention, Lookback Ratio, Head Entropy, Multi-Layer-Attn) decline more gently. This corroborates the mechanistic claim of Section 3.1.2: hidden states encode *prefix-conditional belief*, and the longer the prefix between the contamination and the evaluation turn, the more confidently the model’s belief re-stabilizes around the corrupted narrative—producing hidden states that are *more* coherent with the wrong prefix, not less. Attention features, by contrast, capture structural routing patterns that depend on *how* the model is processing the current turn rather than on *how long ago* the error occurred, and are therefore less sensitive to d .

PAIR itself remains among the top performers across all distances and exhibits the smallest drop with d : on ToolBench it holds near 0.80 accuracy even at $d = 7+$, where every hidden-state probe has fallen below 0.70. This robustness is a direct consequence of PAIR’s two-stage design—when s_{bc} becomes unreliable at long distances, the attention-based correction head detects the structural anomaly and shifts s_{final} accordingly—and extends the contamination asymmetry of Section 3.1.2 along a new axis: the *temporal distance* between the corruption and the step being scored, not just the presence or absence of contamination.

C Training & Inference of PAIR

C.1 training

PAIR requires a one-time offline training procedure:

1. **Data:** We use a balanced dataset of clean and contaminated trajectories with binary correctness labels for each evaluation turn.
2. **Stage 1:** Fit the hidden-state probe on mixed (clean + contaminated) data: `probe_base.fit(H, y)`.
3. **Intermediate:** Compute s_{bc} for all training samples.
4. **Stage 2:** Fit the attention-based correction head on the same data: `probe_correction.fit([A; sbc], y)`.

Both stages use `StandardScaler` normalization and ℓ_2 -regularized logistic regression with $C = 0.01$ (strong regularization to handle the high-dimensional, limited-sample setting).

C.2 Inference as Step-Level Reward

During GRPO training, at each agent step t :

1. The policy generates action a_t with `output_hidden_states=True` and `output_attentions=True` (these are already computed during generation).
2. Extract \mathbf{h}_t (last-token hidden state) and \mathbf{a}_t (multi-layer attention statistics) from the forward pass.
3. Compute $s_{bc} = \text{probe_base}(\mathbf{h}_t)$ and $s_{final} = \text{probe_correction}([\mathbf{a}_t; s_{bc}])$.
4. Assign $r_t = s_{final}$ as the step-level reward at the last token of the assistant turn.

D Ablation Study for Attention Statistics

PAIR’s Stage 2 summarizes each attention head with four statistics (Section 3): `max_attn` (the peak attention value across the head’s attention distribution—“how focused is this head?”), `std_attn` (the spread of that distribution—“how sharp/peaky is it?”), `prefix_ratio` (the fraction of attention directed at prefix tokens—“lookback intensity”), and `self_ratio` (the fraction directed at current-turn tokens—“self-attention within the current turn”). To identify which of these statistics carry the most signal, we re-train the Stage 2 correction head on every non-empty subset of the four statistics and report the resulting probe AUROC on GTA and ToolBench (Figure 6), and three patterns emerge.

First, `std_attn` is the weakest signal on its own, dropping to 0.749 AUROC on ToolBench (vs. 0.822 for `prefix_ratio` or `self_ratio`) and to 0.885 on GTA (vs. 0.908 for `max_attn`). Distributional sharpness alone—absent any information about *where* that attention is directed—carries little discriminative content.

Second, the two “routing” statistics `prefix_ratio` and `self_ratio` are the most consistently informative across both benchmarks: each alone matches the full four-feature combination on ToolBench (0.822 vs. 0.824) and is within 0.005 of the best single feature on GTA. This is consistent with the mechanistic story of Section 3.1.2: attention features are robust to prefix contamination because they encode *which tokens the model attends to*, not merely *how peaky* that attention is. A correct repair turn and an error-perpetuating turn can produce equally sharp attention distributions; what distinguishes them is whether attention reaches into task-relevant context.

Third, combining the four statistics yields only a marginal gain over the strongest individual one—the full set reaches 0.910 / 0.824 versus 0.908 / 0.822 for the best single feature—indicating diminishing returns within this feature family. PAIR therefore extracts most of its attention-side signal from a small number of structural *routing* statistics, and the design is robust to the precise choice of features within the four-statistic family.

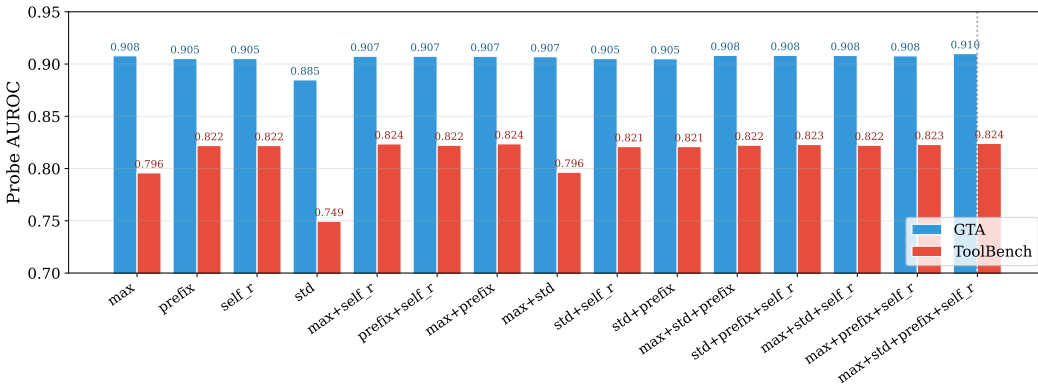


Figure 6: Ablation over the four attention statistics in PAIR’s Stage 2.

E Detailed Reward Design with PAIR

Saturation-controlled probe score. To prevent the base PAIR score from collapsing to $\{0, 1\}$ during training—which would zero out the group variance regardless of any momentum bonus—we first transform $s_{final,t}$ with a temperature-clipped sigmoid:

$$\tilde{s}_{final,t} = \text{clip}\left(\sigma\left(\frac{1}{T} \logit(s_{final,t})\right), \varepsilon, 1 - \varepsilon\right), \quad (5)$$

with $T = 2$ and $\varepsilon = 0.05$. The temperature softens overconfident probe outputs, and the hard clip at ε ensures $\tilde{s}_{final,t}$ stays away from the exact endpoints, guaranteeing positive group variance throughout training. All subsequent quantities are computed from $\tilde{s}_{final,t}$ rather than the raw $s_{final,t}$.

Momentum-based reward. Define the running mean of PAIR scores over the prefix as

$$\bar{s}_{<t} = \begin{cases} \tilde{s}_{final,1} & \text{if } t = 1, \\ \frac{1}{t-1} \sum_{j=1}^{t-1} \tilde{s}_{final,j} & \text{if } t \geq 2. \end{cases} \quad (6)$$

The step-level reward is then

$$r_t = \sigma\left(\text{logit}(\tilde{s}_{final,t}) + \alpha \cdot (\tilde{s}_{final,t} - \bar{s}_{<t})\right), \quad (7)$$

where $\alpha > 0$ is a scaling hyperparameter (we set $\alpha = 5$), and we refer to the additive term $b_t = \alpha(\tilde{s}_{final,t} - \bar{s}_{<t})$ as the *momentum bonus*. By construction, the first turn receives no momentum bonus ($r_1 = \tilde{s}_{final,1}$), and from $t = 2$ onward the bonus contrasts the current step against the running mean of all earlier steps.

The momentum term $\tilde{s}_{final,t} - \bar{s}_{<t}$ is *symmetric*: when the current step exceeds the trajectory’s running mean it receives a positive logit-space boost, and when it falls below the running mean, it is penalized correspondingly.

Adding the bonus in *logit space* rather than directly in score space has two practical benefits. First, r_t is guaranteed to remain in $(0, 1)$ for any value of α and b_t : a logit-space sum maps via $\sigma(\cdot)$ back into the valid reward range without clipping. Second, the construction inherits the natural saturation of the sigmoid: when $\tilde{s}_{final,t}$ approaches 0 or 1, its logit moves to $\pm\infty$, so a fixed-magnitude bonus produces a smaller change in the final r_t . This means already-confident probe outputs are perturbed only modestly, while uncertain outputs (with $\tilde{s}_{final,t}$ near 0.5) are most responsive to the momentum signal. The momentum formulation has two practical effects on GRPO training. First, two trajectories in the same group with similar *average* PAIR scores but different per-step *trends* receive different rewards, restoring within-group variance and preventing advantage collapse. Second, the reward explicitly encourages the policy to make each step better than the trajectory so far, which provides a denser learning signal than the absolute PAIR score alone.

Cost. The reward retains PAIR’s probe-level inference cost: \mathbf{h}_t and \mathbf{a}_t are produced as byproducts of the policy’s generation forward pass, the running mean $\bar{s}_{<t}$ updates in $\mathcal{O}(1)$ per step, and Eq. 5–7 reduce to a handful of scalar operations. The Stage 1 and Stage 2 probes themselves are trained once on the offline corpus described in Appendix A *before* GRPO training begins and remain frozen for the entire RL run; we do not re-train or update them during training.

F Complexity Analysis

We analyze the per-step computational cost of each reward source under the operational regime that matters most: dense step-level reward computation during online GRPO training, where every step of all rollouts requires a reward signal. Table 6 summarizes the per-step latency, the additional GPU forward passes required, and any external API calls.

The hidden states and attention statistics required for PAIR are byproducts of the policy’s generation forward pass; we configure the model with `output_hidden_states=True` and `output_attentions=True` so that no additional forward pass is needed. The reward computation itself reduces to two linear transformations of cached activations (one per stage), which take ~ 0.2 ms per step on a single A6000. This is roughly $2,500\times$ faster than an LLM-as-a-judge API call, $150\text{--}250\times$ faster than a teacher-forced log-probability evaluation (IGPO / TIPS), and four to five orders of magnitude faster than tree-search-based methods that issue K sibling rollouts per step. A representative GRPO configuration in our experiments uses batch size 1, group size 4, and a maximum of 10 turns per rollout, yielding up to 40 step-level reward computations per training step and up to 20,000 over 500 training steps. At this scale, the cumulative reward-computation time for PAIR is on the order of a few seconds, while LLM-as-a-judge would require approximately 2.8 hours of GPU-equivalent compute plus the corresponding API expenditure. Tree-based methods are still more expensive: with $K = 4$ sibling rollouts per step (each itself a full multi-turn rollout averaging 5–25 seconds), the cumulative reward-computation cost reaches tens to over a hundred GPU-hours.

The asymmetry compounds at larger training scales. A typical production-style RL configuration (batch size 32, group size 8) issues $\approx 1,500$ reward computations per training step and $\approx 0.77\text{M}$ over 500 training steps. At this scale, PAIR still completes its cumulative reward computation in roughly 2.5 minutes, whereas LLM-as-a-judge would require approximately 107 GPU-hours plus a proportional API bill, and tree-based methods would consume thousands of GPU-hours. The same

Table 6: Per-step cost of each reward source. Latencies are measured on a single A6000 GPU with Qwen2.5-7B-Instruct as the policy. *Additional forward passes* counts forward passes in addition to the policy’s generation pass, which all methods incur. PAIR reuses the activations already produced by the generation pass, so it adds no marginal forward pass.

Reward	Latency / step	Add. fwd passes	External calls	Cost growth
Outcome-only	0 ms	0	×	$O(1)$ per trajectory
Internal probe	~ 0.1 ms	0	×	$O(1)$ per step
IGPO / TIPS	$\sim 30\text{--}50$ ms	1 (teacher-forced)	×	$O(y^*)$
AT ² PO / Tree-GRPO	$\sim 5\text{--}25$ s	K sibling rollouts	×	$O(K)$ per step
LLM-as-a-judge	~ 500 ms	0	GPT-4o-mini	$O(1)$ per step
PAIR(ours)	~ 0.2 ms	0	×	$O(1)$ per step

$2,500\times$ per-call latency advantage of PAIR therefore translates into qualitatively different operating regimes once batch size, group size, multi-seed evaluation, and hyperparameter sweeps are folded in. Beyond per-step cost, PAIR requires a one-time offline training step for the two probes. With 1,600 labeled (clean + contaminated) trajectories per dataset, this fits in approximately 30 s on a single CPU using StandardScaler + ℓ_2 -regularised logistic regression. This cost is amortised across all subsequent training runs: the same probe can be reused across GRPO seeds, hyperparameter sweeps, and training restarts without retraining.

G GRPO Training Configuration

Table 7: GRPO training configuration. All 16 method comparisons share these settings; only the per-step reward function differs.

Setting	Value
<i>Model and fine-tuning</i>	
Base model	Qwen2.5-7B-Instruct
Fine-tuning	LoRA ($r=16$, all projection layers)
Hardware	$2\times$ NVIDIA A6000 (pipeline parallel)
<i>Optimization</i>	
Learning rate	3×10^{-7}
LR schedule	Constant (warmup fraction 0.05)
KL coefficient β	0.01
PPO clip ϵ	0.2
<i>Rollout</i>	
Batch size	1 prompt
Group size G	4 rollouts per prompt
Max turns per rollout	10
Max generation tokens	1024 per turn
Total training steps	500
<i>PAIR-specific</i>	
Probe state	Stage 1 & Stage 2 frozen during RL
Probe re-fitting	Disabled (probe_retrain_every= 0)
Momentum scaling α	5
Temperature T (<code>_temp_clip</code>)	2
Clip endpoints ϵ	0.05

This appendix details the GRPO training configuration used to produce the main results in Table 3 and the cross-domain transfer results in Figure 4. All 16 method comparisons share the same training pipeline; only the per-step reward function (Section 3) differs across methods. The full configuration is summarized in Table 7. Below we explain the empirical reasoning behind the non-default choices.

Small constant learning rate (3×10^{-7}). Larger learning rates—we tested $\{1 \times 10^{-6}, 5 \times 10^{-6}, 1 \times 10^{-5}, 5 \times 10^{-5}\}$ —consistently caused the probe-based reward to saturate within the first 100 training

steps. Once r_t approaches its $\{0, 1\}$ boundaries on every rollout in a group, the GRPO group-relative advantage collapses to near zero and downstream task success drops sharply. The small constant rate of 3×10^{-7} is slow enough that the policy does not learn to fool the probe within the 500-step training budget. We use a constant schedule with 5% warmup; cosine decay was tested but offered no consistent benefit at this small learning rate.

Light KL anchoring ($\beta = 0.01$). The KL coefficient $\beta = 0.01$ acts as a light anchor to the reference policy. Setting $\beta = 0$ (no anchor) produced larger oscillations in the training reward and a single transient peak in validation success; the small positive β flattens the trajectory and produces multiple high-quality intermediate checkpoints (typically near steps 100, 300, and 350) rather than one fragile peak. Larger values ($\beta \geq 0.1$) over-anchor and slow down learning visibly.

Small batch and group sizes. We use batch size 1 with group size $G = 4$, sampling 4 rollouts per prompt for group-relative advantage estimation. This keeps per-step compute manageable on our $2 \times A6000$ pipeline-parallel setup while preserving enough rollout diversity for advantage normalization. Larger group sizes ($G \in \{8, 16\}$) were tested and offered no measurable improvement on GTA at the cost of significantly longer wall-clock per training step.

Long-horizon rollouts. `max_steps_per_rollout` is set to 10, accommodating the full multi-turn structure of GTA and ToolBench without truncation. Generation length per turn is capped at 1024 tokens, sufficient for the Thought / Action / Action-Input format used in both benchmarks.

Frozen probes during RL. Both Stage 1 (belief-consistency estimator) and Stage 2 (attention-based correction head) of PAIR are fit once on the offline corpus described in Appendix A *before* GRPO training begins, and remain frozen throughout the entire RL run. We tested periodic re-fitting of the Stage 2 head on policy-generated trajectories (`probe_retrain_every` > 0) in preliminary experiments; this did not improve performance on GTA and added non-trivial training overhead, so we disable it for the main runs.

PAIR-specific reward parameters. The momentum scaling $\alpha = 5$ in Eq. 7 was selected via sweep over $\alpha \in \{1, 2, 5, 10, 20\}$ on GTA: $\alpha = 5$ produced the most consistent training dynamics (multiple high-quality checkpoints) at $\beta = 0.01$, with smaller α giving weaker momentum signal and larger α inducing instability. The temperature $T = 2$ and clip range $\varepsilon = 0.05$ in Eq. 5 were chosen to prevent the base PAIR score from saturating at $\{0, 1\}$ during training; their values were stable across the sweep and we did not tune them per dataset.

H Detailed Evaluation Process

We evaluate every method on both GTA and ToolBench using a single evaluation pipeline that loads the trained LoRA adapter onto the same backbone (Qwen2.5-7B-Instruct), rolls out the policy on each benchmark’s held-out test split with deterministic decoding, and applies a benchmark-specific scoring function. The protocol mirrors the conventions of the upstream releases of GTA [19] and ToolBench [13] wherever those conventions are publicly documented; the small operational deviations we make are dictated by reproducibility constraints (e.g., deprecated or paid APIs) rather than by our method, and apply identically to all 16 methods compared in Section 4.

Common pipeline. Each rollout follows the standard ReAct format used throughout the paper—an alternation of *Thought*, *Action*, *Action Input*, and *Observation* blocks, terminating either when the policy emits *Final Answer* or when the per-rollout step budget of 10 is reached, matching the upstream GTA evaluation script. Each policy output is first parsed with a regular-expression matcher; on ToolBench, well-formed but slightly off-pattern outputs additionally fall back to a single GPT-4o-mini parsing call. This fallback affects a small fraction of outputs and is enabled identically for every method.

GTA: tool execution and scoring. GTA’s reference evaluator exposes a hybrid tool-execution backend, which we replicate verbatim: tool calls are first matched against a cache built from each test episode’s gold dialog (an exact $(tool_name, canonical\ args) \rightarrow response$ map), then routed to dedicated GPT-4o handlers for the OCR and search tools (matching the reference convention), and only fall back to live `agentLego` execution on a cache miss. This caching is the upstream-prescribed evaluation protocol and ensures that any two methods that emit the same tool call observe exactly the same tool response; it does *not* hide information from the policy. For final-answer scoring we use the upstream `evaluate_answer` routine in its loose-matching mode, which reproduces the `match_answer` function of GTA’s reference script. When the gold answer is a structured `whitelist/blacklist`

dictionary, the score is 1 if at least one whitelist group is fully substring-matched in the prediction and no blacklist phrase appears, and 0 otherwise; when the gold answer is a list of free-form references, we report the maximum cosine similarity between the prediction and the references using `all-mpnet-base-v2` embeddings, again following the reference convention. Following the same upstream convention, episodes whose gold answer is a raw image-file path (the GTA *image-compare* subset, where comparing a textual prediction against a filename is not informative) are excluded from the score; this leaves 53 scored episodes per method, identical to the count used in upstream baselines.

ToolBench: offline replay simulator. ToolBench’s tool surface is a snapshot of more than 16,000 RapidAPI endpoints, a substantial fraction of which are now deprecated, paywalled, or rate-limited. To make evaluation reproducible across methods and seeds, we implement an *offline replay simulator* that resolves every tool call against a cache built from each episode’s gold dialog—the same kind of cache used by GTA’s evaluator, applied to ToolBench’s larger tool inventory. On an exact (*tool_name*, canonical args) hit, the cached response is returned. On a miss, an optional fuzzy fallback selects the cached entry for the same tool whose argument tokens have the highest Jaccard overlap with the policy’s call; this resolves benign argument-formatting differences (e.g., key ordering, trivial extra fields, casing) so that semantically equivalent calls are treated identically. If both the exact and fuzzy lookups miss, the simulator returns a transparent error of the form “[Simulator] Tool ‘X’ with args ... has no cached response”, allowing the policy to recover by issuing a different call rather than silently substituting a fabricated response. We additionally cap the rollout history at 6,000 characters to fit Qwen2.5-7B’s pipeline-parallel forward pass within the memory budget of our hardware ($2 \times A6000$); this limit only takes effect on a small minority of unusually long trajectories and is applied uniformly across all methods.

ToolBench: scoring. ToolBench’s gold answers are verbatim long-form responses produced by ToolLLaMA on RapidAPI’s actual outputs at dataset-collection time. Because these gold strings rarely align with the surface form of an independent model’s free-form answer, exact-substring scoring on the official whitelist returns near-zero scores for *every* method we tested (≤ 0.03 on AT²PO, CoE-C, LLM-as-a-judge, and our own runs), losing all discriminative power. We therefore follow recent ToolBench-style evaluations and adopt an LLM-judge scoring protocol with partial credit. A single GPT-4o-mini call compares the policy’s final answer against the gold answer’s key facts (named entities, numerical values, dates, and stated relations) and returns one of three labels: *yes* (1.0, most key facts captured; formatting differences acceptable), *partial* (0.5, some key facts captured, with minor omissions or local errors), or *no* (0.0, refusal, empty, off-topic, or majority-incorrect). Binary scoring is essentially $\{0, 1\}$ but heavily skewed to 0 on this benchmark and hides all method-level signal; partial-credit scoring resolves the same population into a usable 0.34–0.41 range across the 16 methods. The judging prompt is fixed across all methods and seeds, the system prompt enforces strict JSON output, and the prompt is reproduced verbatim in Figure 10.

LLM-judge as scorer vs. as baseline reward. GPT-4o-mini appears in two distinct roles in our paper, and we keep them strictly separate. (i) As the *evaluation scorer* on ToolBench (this section), GPT-4o-mini receives only the task prompt, the gold answer, and the policy’s final answer, and returns a single yes/partial/no label. This call is invoked identically for every method we score—including the LLM-as-a-judge baseline—so the scorer cannot favor one method over another. (ii) As the *LLM-as-a-judge baseline* (Section 4, Figure 10), GPT-4o-mini receives the full per-step trajectory and returns a 1–10 score *at every step* that is fed back into GRPO as the training reward. The two prompts and the two operating regimes are different, and the evaluation scorer is applied to the LLM-as-a-judge baseline under exactly the same protocol it uses for PAIR and every other baseline. There is therefore no self-comparison or coupling between the scorer and any of the methods being scored.

Aggregation. For each (method, dataset, seed) triple we report the mean score across scored episodes (`mean_score`) and the fraction of episodes with a score of at least 0.5 (`success_rate_at_0.5`). All headline numbers in the main paper are reported as mean over three seeds ($\{42, 43, 44\}$); standard deviations appear in the corresponding result tables.

I Hyperparameter Analysis

The momentum-based reward of PAIR introduces a single new hyperparameter, α in Eq. 7, and our GRPO setup adds two further sensitive choices (KL coefficient β and learning rate). We sweep all three on GTA and report the resulting peak performance in Figure 7. The full sweep covers $\alpha \in \{1, 2, 5, 10, 20\}$, $\beta \in \{0, 0.01\}$, and $\text{lr} \in \{3 \times 10^{-7}, 1 \times 10^{-6}\}$. All other settings are fixed at the canonical values in Table 7.

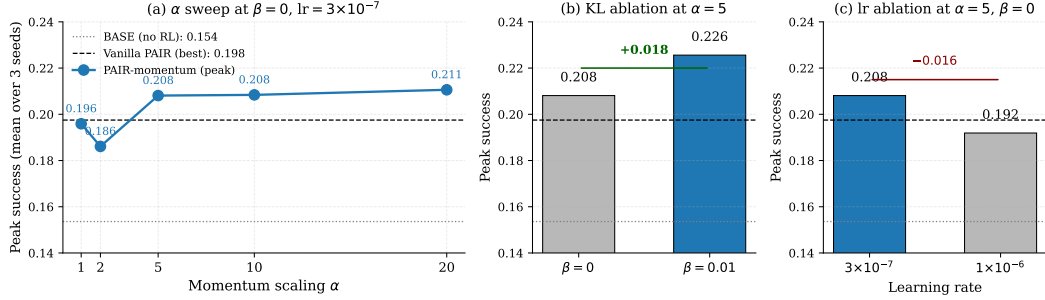


Figure 7: **Hyperparameter analysis on GTA.** (a) Peak PAIR-momentum success as a function of the momentum scaling α at fixed $\beta = 0$, $\text{lr} = 3 \times 10^{-7}$. The sweet spot lies at $\alpha \in \{5, 10, 20\}$, all comfortably above the strongest vanilla PAIR baseline (dashed line); $\alpha \leq 2$ provides too little momentum signal to recover the within-group variance needed for GRPO advantage estimation. (b) A small KL anchor $\beta = 0.01$ improves peak success by +0.018 over $\beta = 0$ at fixed $\alpha = 5$. (c) A larger learning rate 1×10^{-6} reduces peak success by 0.016 relative to 3×10^{-7} at fixed $\alpha = 5$, $\beta = 0$, and yields a more chaotic per-step trajectory. Reference horizontals: BASE (no RL training, dotted) and the strongest vanilla-PAIR run (dashed).

Momentum scaling α . Figure 7(a) reports peak PAIR-momentum success as a function of α at fixed $\beta = 0$ and $\text{lr} = 3 \times 10^{-7}$. Performance is weak at $\alpha \leq 2$ (0.196 for $\alpha = 1$, 0.186 for $\alpha = 2$), rises sharply at $\alpha = 5$ (0.208), and stays in the same range up to $\alpha = 20$ (0.211). Below $\alpha = 5$ the momentum signal is too weak to recover the within-group variance lost to probe-output similarity (Section 3); above $\alpha = 20$ we observed early-stage instability without a corresponding headline gain. The $\alpha \in \{5, 10, 20\}$ plateau also indicates that PAIR is not sensitive to the precise value of α , only to its order of magnitude. We adopt $\alpha = 5$ for all main results.

KL anchor β . Figure 7(b) compares $\beta = 0$ and $\beta = 0.01$ at fixed $\alpha = 5$ and $\text{lr} = 3 \times 10^{-7}$. The small KL anchor improves peak success by +0.018 (0.208 \rightarrow 0.226) and, in our per-step trajectories, produces multiple stable high-scoring checkpoints rather than the single sharp peak observed at $\beta = 0$. Larger values ($\beta \geq 0.1$) over-anchor and slow down learning visibly without further stability benefit. We use $\beta = 0.01$ throughout.

Learning rate. Figure 7(c) compares the two learning rates at fixed $\alpha = 5$ and $\beta = 0$. Increasing the learning rate from 3×10^{-7} to 1×10^{-6} reduces peak success by 0.016 (0.208 \rightarrow 0.192) and produces a more chaotic per-step trajectory with a sharp early dip. Larger learning rates ($\geq 5 \times 10^{-6}$) caused the probe-based reward to saturate at $\{0, 1\}$ within 100 steps and the GRPO group-relative advantage to collapse, an outcome we discuss further in Appendix G. We use $\text{lr} = 3 \times 10^{-7}$ throughout.

Best-checkpoint selection. The sweep above is axis-aligned: α is varied at $\beta = 0$ and $\text{lr} = 3 \times 10^{-7}$; β is varied at $\alpha = 5$ and $\text{lr} = 3 \times 10^{-7}$; lr is varied at $\alpha = 5$ and $\beta = 0$, yielding nine PAIR-momentum runs in total. Across these nine runs, the highest-scoring checkpoint lies at step 50 in three runs, between steps 100–400 in five runs, and at step 450 in one run; *not a single run* reaches its best at step 500. Reporting only the final checkpoint would systematically underestimate any method that exhibits oscillation under probe-based reward, including PAIR. We therefore evaluate every checkpoint saved at 50-step intervals and report the best-scoring one for all main results, and we recommend the same protocol for any future work using internal-probe step-level rewards.

J Limitation and Future Work

We discuss limitations of the present work and concrete avenues for follow-up.

Backbone model scope. Our experiments use a single backbone model (Qwen-2.5-7B-Instruct) for the main results. We do not establish how the belief-consistency bias scales with backbone size or family. Extending the analysis to architectures with different attention designs (e.g., Llama-style GQA, Mistral-style sliding window), to larger scales (e.g., 32B+) is a natural next step.

Beyond binary correctness labels. Our offline corpus uses binary correctness labels at the evaluation turn. Many agentic settings have richer feedback structures—partial-credit progress measures, tool-output utility, or human-graded preference rankings—that could supervise a more nuanced

reward head. Combining PAIR’s probe-level efficiency with such graded supervision is a promising direction for getting denser learning signal without sacrificing the practical cost profile that makes PAIR deployable in the first place.

Broader impact. PAIR accelerates RL training of multi-turn LLM agents by replacing external reward sources (LLM judges, ground-truth queries) with a probe over the agent’s own internal state. This lowers the cost barrier to training capable autonomous agents, which carries the standard dual-use risks associated with more capable agentic LLMs, including misuse for automated phishing, fraud, or unauthorized data exfiltration through tool APIs. We do not introduce new attack surfaces beyond those already present in the underlying base model, but we encourage downstream practitioners to pair training-time efficiency gains with corresponding investments in deployment-time safety filters, capability evaluations, and monitoring of tool-use behavior.

K Prompts

This appendix reproduces the prompts used elsewhere in the paper, both for the offline data construction pipeline that underlies our motivation experiments and for the baseline reward methods we compare against.

Contamination generation. The matched clean / contaminated trajectory pairs used in the motivation experiments (Section 3.1.2) and in PAIR’s offline training corpus (Appendix A) are produced by GPT-4o-mini using a pair of type-specific prompts. Figure 8 reproduces the four *system* prompts—one per contamination type (`reasoning_error`, `tool_misuse`, `observation_misinterpretation`, `stale_memory`)—each instructing the model to inject a subtle and locally plausible error of the corresponding kind into a target assistant turn. Figure 9 reproduces the corresponding *user* prompts, which supply the conversation context, the target turn to be modified, and (for `observation_misinterpretation`) the preceding tool observation. The combination of these system and user prompts is what produces the contaminated turns referenced throughout the paper.

LLM-as-a-judge baseline. The LLM-as-a-judge baseline issues a per-step API call to GPT-4o-mini using the system and user prompts shown in Figure 10. The judge receives the task description and the trajectory up to (and including) the turn being scored, and is asked to return a single integer in $[1, 10]$ as a JSON object. We normalize this score to $[0, 1]$ and use it as the per-step reward whenever the LLM-as-a-judge baseline is invoked.

System Prompt
<p>**reasoning_error** You are an expert at creating subtle reasoning errors in AI assistant responses. Given an assistant's response within a multi-turn conversation, modify it so that the logical reasoning or conclusion is WRONG, but the error is subtle and plausible. The response should sound confident and natural — not obviously nonsensical. Keep the same tone, format, and length. Change the reasoning or conclusion to reach a wrong answer. Only modify the specific turn provided, not others. Return ONLY the modified turn content as a JSON object with the same keys as the original.</p>
<p>**tool_misuse** You are an expert at creating subtle tool misuse errors in AI assistant actions. Given an assistant's tool call within a multi-turn conversation, modify it so that the tool is called with WRONG arguments (e.g., wrong file, wrong parameter value) or a WRONG tool is chosen. The error should be plausible — something a careless assistant might actually do. Keep the same format. Return ONLY the modified turn content as a JSON object with the same keys as the original.</p>
<p>**observation_misinterpretation** You are an expert at creating subtle observation misinterpretation errors. Given a tool observation and the subsequent assistant response, modify the assistant's response so that it MISINTERPRETS the tool output. The tool output stays unchanged. The misinterpretation should be plausible — e.g., reading the wrong value, confusing units, swapping items, or drawing an incorrect conclusion from correct data. Return ONLY the modified assistant turn content as a JSON object with the same keys.</p>
<p>**stale_memory** You are an expert at creating subtle stale memory errors in AI conversations. Given a multi-turn conversation and a specific assistant turn, modify that turn to include a statement or assumption that CONTRADICTS information established in earlier turns. The contradiction should be subtle — e.g., using an outdated value, referencing a wrong earlier result, or misremembering a previous step. Keep the same format. Return ONLY the modified turn content as a JSON object with the same keys as the original.</p>

Figure 8: System prompts driving the GPT-4o-mini contamination generator.

User Prompt
<pre> For `reasoning_error` and `tool_misuse`: ... ## Conversation context (up to the target turn): {context} ## Target assistant turn to modify: {target_json} Apply a subtle '{contamination_type}' to this turn. Return the modified turn as a JSON object. ... For `observation_misinterpretation`: ... ## Conversation context (up to the target turn): {context} ## Preceding tool observation: {tool_json} ## Target assistant turn to modify (misinterpret the observation above): {target_json} Modify the target assistant turn so it misinterprets the tool observation. Return the modified turn as a JSON object. ... For `stale_memory`: ... ## Full conversation context: {context} ## Target assistant turn to modify (inject stale/contradictory memory): {target_json} Modify this turn to include a subtle reference to information from earlier turns that is WRONG or outdated. Return the modified turn as a JSON object. ... </pre>

Figure 9: User prompts driving the GPT-4o-mini contamination generator.

System Prompt
You are a strict JSON-only evaluator.
User Prompt
<pre> You are evaluating a multi-turn agent on a task. Task: {task} Trajectory so far (through the turn to evaluate): {history} Rate the LAST assistant turn on a 1-10 scale: - 10: meaningfully advances the task toward success - 1: wrong, wasteful, or harmful to task progress Return ONLY a JSON object: {"score": <int 1-10>} </pre>

Figure 10: Prompts for GPT-4o-mini to judge the score of each trajectory step.